applied sciences

MDPI

Article

# Real-Time Compensation for Thermal Errors of the Milling Machine

**Tsung-Chia Chen [1,*], Chia-Jung Chang [1], Jui-Pin Hung [2], Rong-Mao Lee [1] and Cheng-Chi Wang [2]**

[1] Department of Mechanical Engineering, National Chin-Yi University of Technology, Taichung 41170, Taiwan; arish.man@msa.hinet.net (C.-J.C.); maxmou@ncut.edu.tw (R.-M.L.)

[2] Ph.D. Program, Graduate Institute of Precision Manufacturing, National Chin-Yi University of Technology, Taichung 41170, Taiwan; hungjp@ncut.edu.tw (J.-P.H.); wcc@ncut.edu.tw (C.-C.W.)

* Correspondence: ctchen@ncut.edu.tw; Tel.: +886-4-2392-4505 (ext. 7154); Fax: +886-4-2393-0681

Academic Editor: Takayoshi Kobayashi

Received: 30 November 2015; Accepted: 28 March 2016; Published: 7 April 2016

**Abstract:** This paper is focused on developing a compensation module for reducing the thermal errors of a computer numerical control (CNC) milling machine. The thermal induced displacement variations of machine tools are a vital problem that causes positioning errors to be over than 65%. To achieve a high accuracy of machine tools, it is important to find the effective methods for reducing the thermal errors. To this end, this study first used 14 temperature sensors to examine the real temperature fields around the machine, from which four points with high sensitivity to temperature rise were selected as the major locations for creating the representative thermal model. With the model, the compensation system for controlling the displacement variation was developed. The proposed model has been applied to the milling machine. Current results show that the displacement variations on the *x*- and *y*-axes and the position error at the tool center were controlled within 20 μm when the compensation system was activated. The feasibility of the compensation system was successfully demonstrated in application on the milling operation.

**Keywords:** thermal modeling; thermal error compensation; machine tool

## 1. Introduction

Position accuracy is one of the critical performance factors affecting the machining precision of machine tools in operation. According to the studies [1,2], thermal deformations may be responsible for 40%–70% of geometrical inaccuracies of machine tools. To reduce the influence of the thermal induced errors, some techniques associated with the compensation schemes have been developed and implemented in the machine tools, including implementation of thermally symmetrical machine design [3–5], the introduction of additional cooling systems [6,7] and thermal deformation compensation [8–10]. Although optimization designs of machine tool structure are an effective way to reduce thermal errors, thermal displacement cannot be completely avoided since the external and internal heat sources under varying operating conditions cannot be accurately predicted at the design stage. Compensation techniques are considered essential methods for reducing the positioning errors and hence increasing the working accuracy [11,12]. Thermal problems are more complicated than geometric problems because the temperature field of a machine tool changes constantly with the working cycle and the environmental conditions. The development of an effective thermal error compensation system greatly depends on the accurate prediction of the time-variant thermal errors. Most thermal error compensation studies have focused on the measurements of the thermal characteristics and then the establishment of thermal-induced error models with accurate prediction based on empirical approach [13–15]. Generally, the most common model for prediction of thermally induced displacements is obtained by multiple linear regressions [16,17]. Recently, different kinds of

artificially intelligent approaches have also been applied to thermal error modeling in order to improve the accuracy and robustness of the error models. These artificial intelligence modeling techniques include artificial neural networks (ANNs) [18–20], fuzzy logic [19], adaptive neuro-fuzzy inference systems (ANFIS) [21] and integrations of the different modeling methods [22,23]. For example, Vanherck *et al.* [18] applied the artificial neural network model to approximate complex multivariable non-linear relationships and hence effectively compensated for the thermal deformation of multiple axes machine tools. Their results showed the maximum deformation was reduced from 150 μm to 15 μm, and the machining error was reduced from 75 μm to 16 μm through the application of the neural model. Horejša *et al.* [24] employed thermal transfer functions to develop an advanced thermal compensation in horizontal four-axis machine tools. Only four thermal sensors, instead of 21 original sensors, were used for calibration of measurements, which were found to decrease the error from 100 μm to 10 μm, and lessen the displacement error of the tool center point.

In more recent years, Abdulshahed *et al.* [22] proposed a novel method combining the ANFIS and grey system theory to predict thermal errors in machining. Basing on this method, they further developed accumulation generation operation (AGO) to simplify the modeling procedures, which were demonstrated to have a stronger prediction power than the standard ANFIS model. In another work [23], they integrated the adaptive neuro fuzzy inference system (ANFIS) with fuzzy c-means clustering method (FCM) to forecast thermal error compensation on computer numerical control (CNC) machine tools. Results of their studies show that the ANFIS-FCM model produced better performance, achieving up to 94% improvement in errors with a maximum residual error of $\pm 4$ μm.

Another important factor affecting the accuracy in thermal error modeling is the temperature variables, which are determined based on selection of appropriate locations for the temperature sensors. Basically, the location and number of sensors are determined based on engineering experience, often placing the sensors near the heat sources [25–27], or selecting them by using statistical techniques [28], and decomposition methods [29]. Generally, the optimum decisions in the location and numbers for temperature sensors are often not practical to machine users because of the different operating conditions in machining and environments of different machine. For this, Abdulshahed *et al.* [30] employed grey system theory to assess the influence weightings of all possible temperature sensors on the thermal response of the machine structure, which were further clustered into groups using the fuzzy c-means (FCM) clustering method. By this method, the number of temperature sensors was reduced from 76 possible locations to five, which significantly minimized the computational time, cost and effect of sensor uncertainty. In study of Abdulshahed *et al.* [31], they proposed a thermal model combining the Grey model GM(0, N) and the ANFIS model, and the temperature variables were recorded through the thermal imaging camera which had high pixel resolutions equating to 76,000 possible temperature measurement points, hence reducing the number of temperature locations to the equivalent of 525 points. This method can be applied to find the optimal location for temperature measurement when designing a thermal error control model.

In this study, thermal error model analysis and robust modeling were developed to control the thermal induced positioning error of a CNC milling machine. To create the thermal model, the locations of four thermal sensors were appropriately selected to establish the thermal displacement prediction model based on the initial measurements with the use of 14 sensors. Finally, the proposed compensation system was developed and implemented in a three-axis milling machine. The feasibility of the compensation system was validated through the application of milling operation.

## 2. Thermal Model of a Machine Tool

### *2.1. Basic Theory*

There are three ways for transmitting the heat from one site to another in a structure.

1. Heat Conduction: heat can transfer from higher temperature to a lower one mainly by means of the solid medium, which can be described by following equation:

$$q = kA\frac{\mathrm{d}X}{\mathrm{d}T} \tag{1}$$

where $q$ is heat conduction, $k$ is conduction factor of the medium, $A$ is the area of contact surface, $\mathrm{d}X$ is the distance between the ends, and $\mathrm{d}T$ is the temperature difference between the ends.

2. Heat convection: heat is delivered naturally from one side to another by affecting the volume and density of the media, which can be described by the following equation:

$$q = hA\Delta T \tag{2}$$

where $q$ is heat convection, $h$ is convection factor, $A$ is sectional area, and $\Delta T$ is temperature difference between the ends.

3. Heat irradiation: Heat is delivered through electromagnetic wave, independent on any media, which can be described by following equation:

$$q = \sigma A(T_1^4 - T_2^4) \tag{3}$$

where σ represents Stefan-Boltzmann constant, $A$ is the radiating surface area, and $T_1$ and $T_2$ are the temperatures at two radiating surfaces.

Generally, there are three kinds of heat sources inducing the thermal deformation (Figures 1 and 2). Firstly, the thermal deformation exists in the rotating spindle and ball-screw, which causes the thermal expansion of the internal components and hence the structure bending deformation of the machine tools. Secondly, there are errors of volume induced from structure construction in assembly error and between different mechanisms. Finally, errors of the controlled system are due to the interpolation errors of the CNC controller or errors of the servo system. These different kinds of errors should be overcome for precision manufacturing industry.

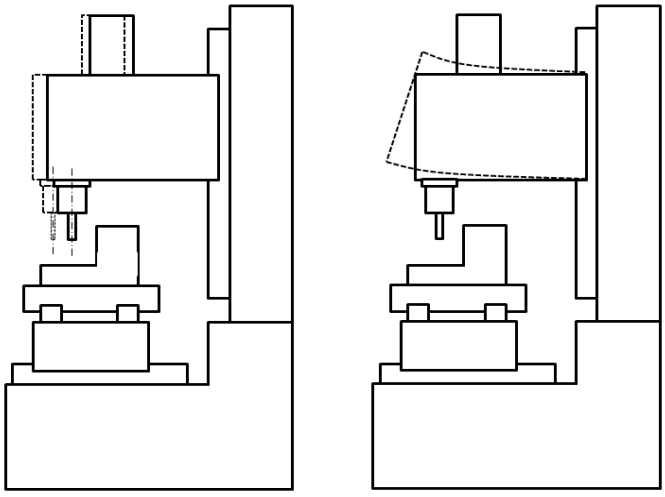

**Figure 1.** Thermal deformation of machine tools.

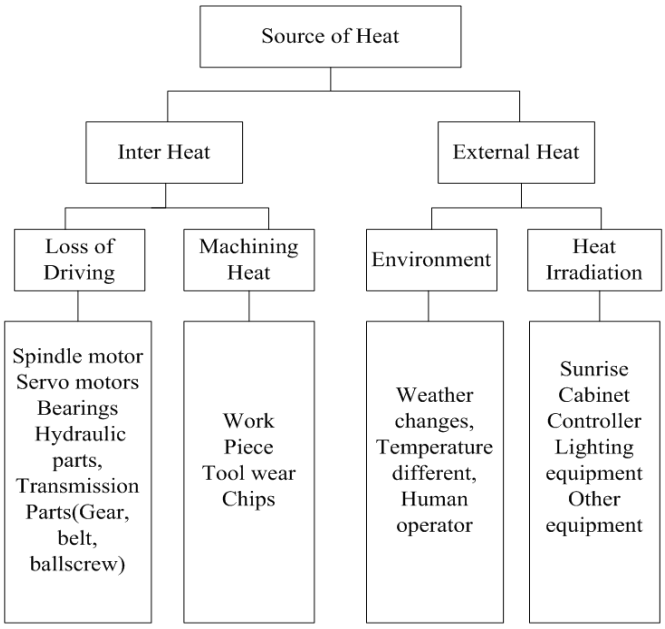


**Figure 2.** Factors inducing thermal deformations.

### *2.2. Thermal Model*

Thermal error identification is one of the crucial steps for a successful thermal error modeling and compensation. It would be a practical thought that the deformations or displacement variations at certain points of machine tools due to thermal error can be obtained by measuring the temperature of the major points on the machine and other possible variables. However, it is a prerequisite to establish a compensation model about the thermal induced variation in displacement. Essentially, there are two methods for establishing the thermal model of the machine tool system [2,6].

#### 2.2.1. Theoretical model

This method was implemented based on the numerical analysis through the finite element approach [5]. Generally, the temperature distributions of a milling machine are predicted based on differential formulas according to the heat transfer analysis. The thermal induced deformations are then calculated based on theory of elasticity through the finite element method. In this model, the determination of possible heat sources existing in different mechanism is prerequisite, but it is a difficult task to obtain the accurate data describing the heat flux generated in the various transmission components, which further results in the unrealistic model for thermal compensation.

#### 2.2.2. Data-driven model

Generally, the thermal model can be practically established based on the collected parameters of the system by means of the different methods, including the statistics model, exponential function, multiple regression, non-linear multiple regression, neural networks, expert system and fuzzy theory.

In this study, the multiple linear regression analysis is employed to describe the correlation between axial deformation and temperatures. Regression analysis is characterized by the general form:

$$\delta = E(\varepsilon, \Delta T_1, \Delta T_2, \ldots\ldots \Delta T_n) \tag{4}$$

The multiple linear regression is defined as a linear combination of several independent variables and one dependent variable in the form:

$$Y = \beta_0 + \beta_1 X_1 + \beta_2 X_2 + \ldots\ldots\ldots\ldots\ldots + \beta_k X_k + \varepsilon \tag{5}$$

where $\beta_i$, $i = 0, 1, 2, \ldots$ is the regression coefficient, $\varepsilon$ is the total truncation errors. This system can also be written in matrix form:

$$\begin{array}{c} [Y] = [X][\beta] + [\varepsilon] \\ y = \beta_0 + \sum_{j=1}^{k} \beta_j X_{ij} + \varepsilon_i \end{array} \quad (6)$$

$$Y = \begin{bmatrix} y(1) \\ y(2) \\ y(3) \\ . \\ . \\ . \\ . \\ y(n) \end{bmatrix} = \begin{bmatrix} 1 & x_1(1) & .... & x_k(1) \\ 1 & x_1(1) & .... & x_k(2) \\ 1 & x_1(1) & .... & x_k(3) \\ . & . & & . \\ . & . & & . \\ . & . & & . \\ . & . & & . \\ 1 & x_1(1) & & x_k(n) \end{bmatrix} \begin{bmatrix} \beta_1 \\ \beta_3 \\ \beta_3 \\ . \\ . \\ . \\ . \\ \beta_k \end{bmatrix} \quad (7)$$

In the above, the regression coefficients can be obtained by using the well known least-squares method.

## 3. Experiment Approach

### *3.1. Experiment Setup*

The milling machine used for experiment was made by the Quaser machine tool company (MV204C) (Taichung, Taiwan), as shown in Figure 3. The main specifications are: a spindle unit of 12,000 rpm, three axes linear guide modules ($X$, $Y$ ball guides and $Z$ roller guide), auto-lubrication system and Heidenhain 530 controller (Heidenhain, Berlin, Germany). Before creating the thermal model, it is necessary to realize the temperature distribution fields of the whole machine. This can also help to determine the critical points associated with the temperature fields dominating the thermal model of the machine.

**Figure 3.** MV204C Quaser machine tools.

### *3.2. Initial Measurement*

In precision machine tools, the main heat sources may come from the cutting process and the transmission mechanism. The heat generated in operation distributed among the workpiece, the chips, and the coolant. The majority of heat (60%–80%) is carried away by chips and eventually will be transferred to the coolant, while the heat sources in the feeding mechanism include the mechanical motion components and electrical driven components. Therefore, considering the milling machine used in this study, 14 temperature sensors were used to be placed at different locations, as shown in Figure 4, including the main heat sources, such as the spindle driven motor, and the other parts such as the vertical column and machine base where the heat can be conducted from heat sources.

The measurement was performed for 48 h under spindle running at 7200 rpm. The temperature rises measured at the 14 points are illustrated in Figure 5. As expected, some major sites near the spindle bearings, transmissions belt and driven motor show significant temperature increments, which can be the candidates for the temperature variables in the thermal model.

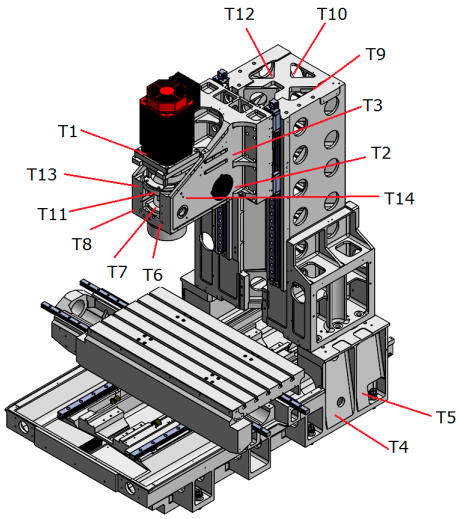


**Figure 4.** Schematics of the initial measurement of temperature fields with 14 sensors.

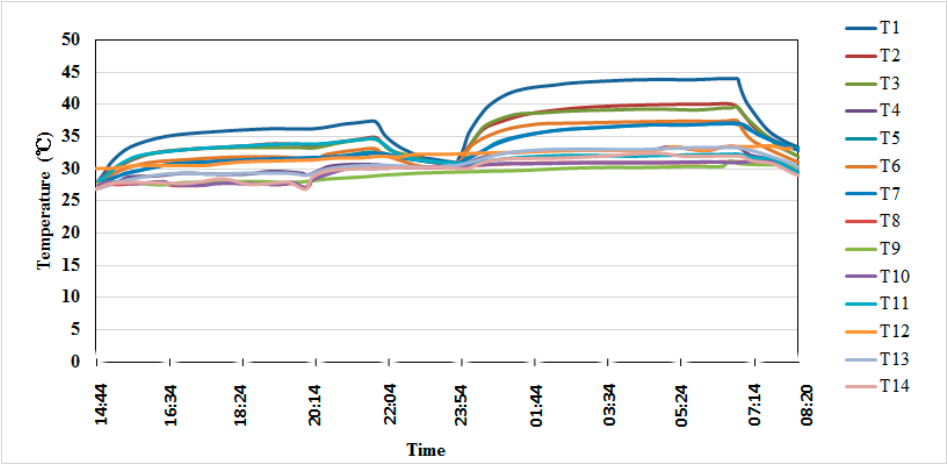


**Figure 5.** Initial temperature rises measured at 14 sensors.

### *3.3. Measurement of Major Temperature Fields*

After the initial measurement, three points were selected to be measured for creating the thermal model. In addition, the fourth point was located at the machine base to measure the environmental temperature as a reference to the temperature fields of the machine. As listed in Table 1, there are four sensors mounted on the machine to capture the required temperature data. The locations of the sensors are shown in Figure 6, in which T1 is located at the rear bearings of the spindle, T2 is located at the heat source of the belt transmission with greater frictional effect between belt and pulleys, T3 is located at spindle motor, T4 is mounted on the machine base where the temperature is controlled at around 28 °C. In addition, four non-contact displacemeters were used to detect the variations of the displacement of the working table along the *x*-, *y*- and *z*-axes (Figure 7). Formal measurement continued after the confirmation of the collecting data for 48 h of spindle running (7200 rpm and 10,800 rpm). The temperature rises measured at the four points are illustrated in Figure 8. From this figure, we can

find that the temperatures measured at points around the spindle head vary significantly with the operating time of spindle, while the temperature variation at the machine base was insignificant. This can be ascribed to the fact that the machine was operated in a temperature-controlled environment, which also reduced the sensitivity of machine structural components to the environment's temperature.

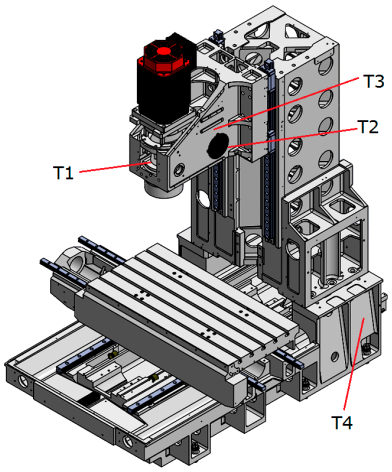


**Figure 6.** Schematics of the locations of temperature sensors.

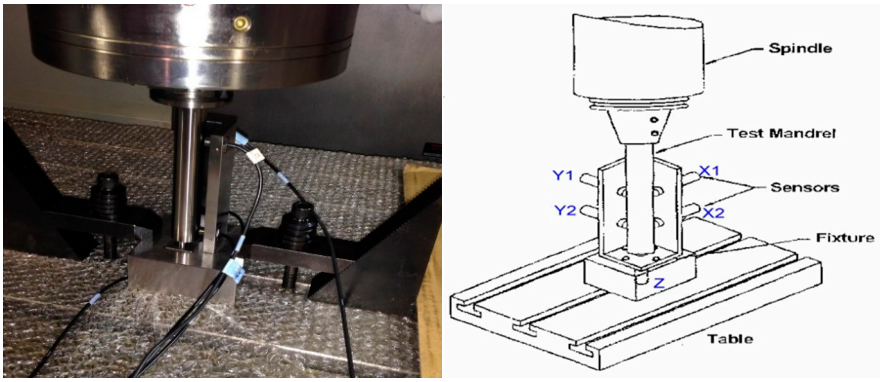


**Figure 7.** Measurement of displacements of working table in *X*, *Y* and *Z* directions.

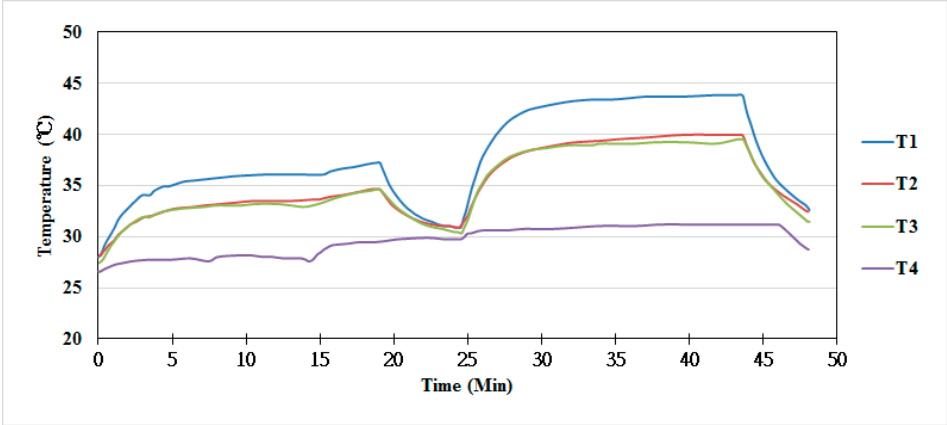


**Figure 8.** Temperature rises with time measured at four sensors.

**Table 1.** Locations of the temperature sensors.

| Temperature Sensor | Locations |
|---|---|
| T1 | Nearby rear bearings of spindle |
| T2 | Heat source of belt transmission in spindle head |
| T3 | Nearby spindle motor (directly) |
| T4 | Machine base, temperature of the environment |

### *3.4. Application of Compensation Module*

Following the above experiments, the thermal model was created based on the major temperature fields measured at the major points and the displacement variations of the working table. Then, the hardware module for compensation of thermal induced error was established, as shown in Figure 9, which mainly consists of the 8-bit microprocessor PIC18F6520 with 32 KB flash rom. The interactive communication and calculation for compensation protocol between data sensors and microprocessor was shown in Figure 10.

To verify the feasibility of the proposed thermal error compensation module in the practice of machining, this system was applied to investigate the positioning precision of the milling machine. The testing procedures are described briefly as follows:

(1) Initial running of spindle for 48 h to ensure the measuring points on the machine tool, which can satisfy the desired temperature fields of thermal model.

(2) Operating the spindle at 60% of full speed for 400 h—then, turning off the spindle and ensuring the *x*-*y* table and the spindle nose return to their initial positions.

(3) Performing the test by running the spindle at 90% of full speed for 400 h, in the meantime, recording the displacements of the table on the *x*- and *y*-axes and spindle nose on the *z*-axis.

(4) Activating the compensation module to remove the displacement error due to temperature rise.

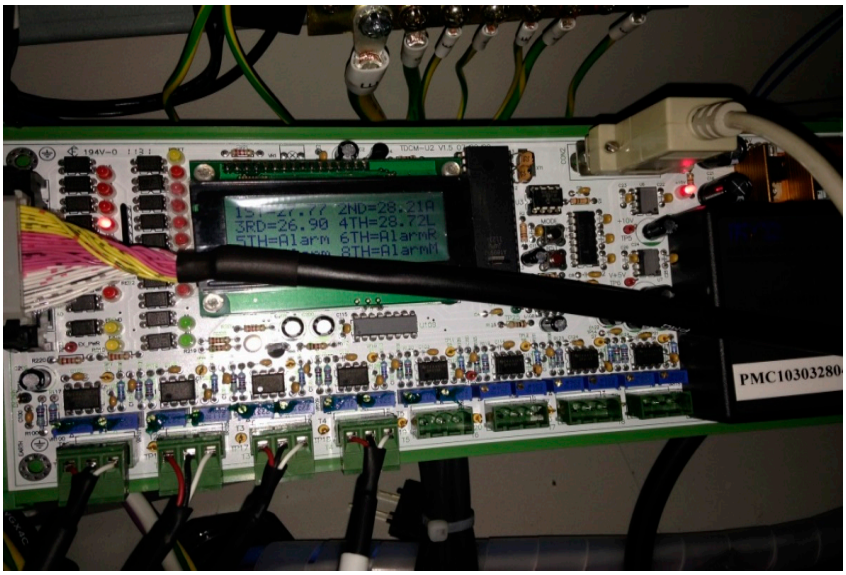


**Figure 9.** Thermal compensation module.

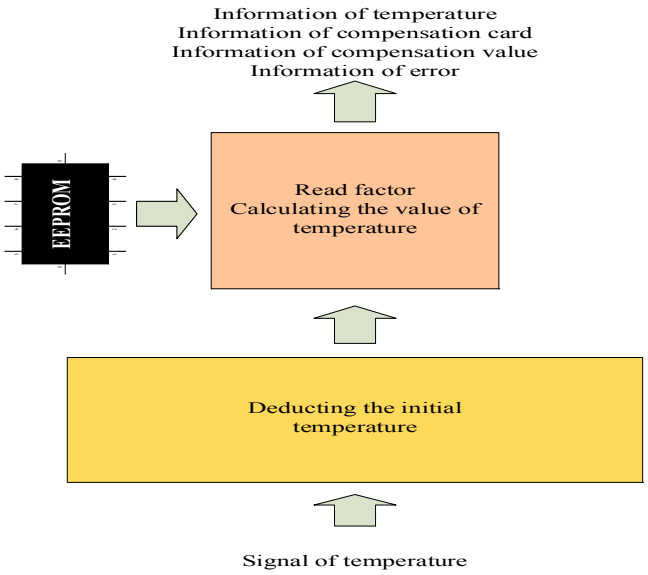


**Figure 10.** Communication module.

## 4. Results and Discussions

### *4.1. Displacement Variation without Compensation*

Figure 11 shows the temperature and displacement variations of the working table on the *x*- and *y*-axes and the spindle nose on the *z*-axis during the 400 h operations. It is found that the *x* and *y* axial displacement variations are within the range of 10–25 μm and 8–20 μm, respectively. While the displacement variation on the *z*-axis is about 70 μm. The greater displacement variation on the *z*-axis can be ascribed to the fact that there is a high temperature rise in the spindle unit running at high speed for a long time. It can be expected that this will result in the poor precisions in machining.

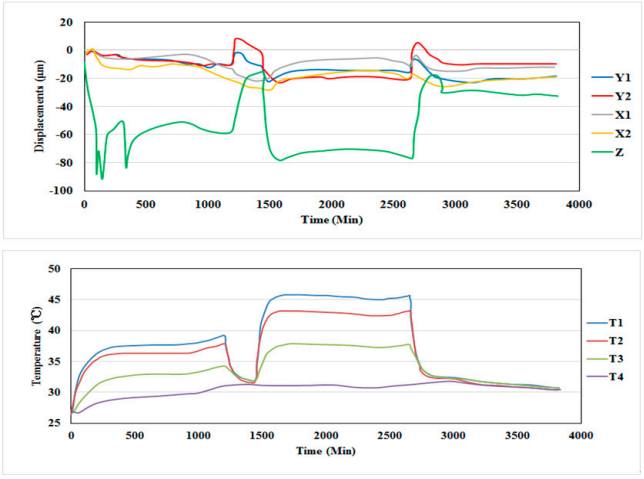


**Figure 11.** Temperature and displacement variations of the working table on the *x*- and *y*-axes and the spindle nose on the *z*-axis during the 400 h operations.

### *4.2. Displacement Variation with Compensation*

Figure 12 shows the temperature and displacement variations on the *x*-, *y*-, and *z*-axes during the 400 h operations when activating the compensation modulus. In this case, we can find that the maximum displacement variations on the *x*- and *y*-axes are within 30 and 20 μm, respectively. While

the displacement variation on the *z*-axis is about 40 μm. It is apparent that the displacement error on the *z*-axis was controlled within a small range by the compensation module.

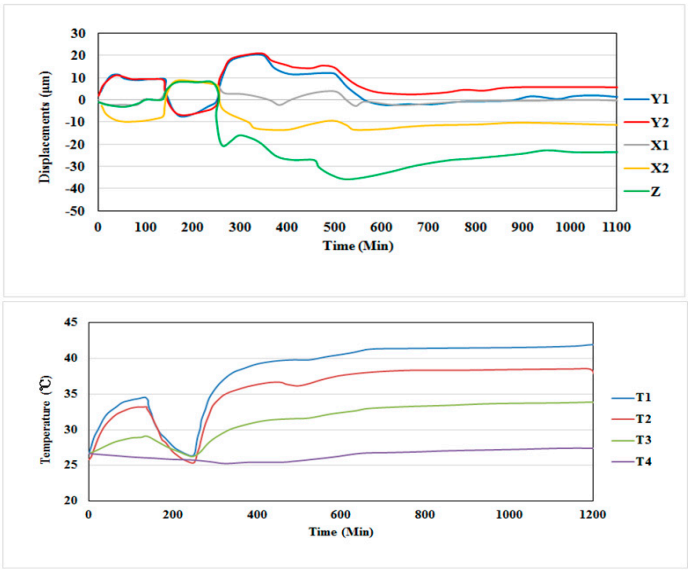


**Figure 12.** Temperature and displacement variations on the *x*-, *y*-, and *z*-axes under the activation of temperature compensation system.

Since the displacement variations on the *y*- and *z*-axes are still beyond the desired range, we adjusted the control parameters of compensation module and conducted the test again following the previous procedures. Figure 13 shows the temperature and displacement variations on the *x*-, *y*-, and *z*-axes during the 400 h operations when activating the modified compensation module. In this case, the maximum displacement variations on the *x*- and *y*-axes are controlled within 14–20 μm and 15–20 μm, respectively. While the displacement variation on the *z*-axis is also controlled below 20 μm approximately. This result again verifies the feasibility of the compensation module to reduce thermal error caused by the temperature rise of the spindle tooling system.

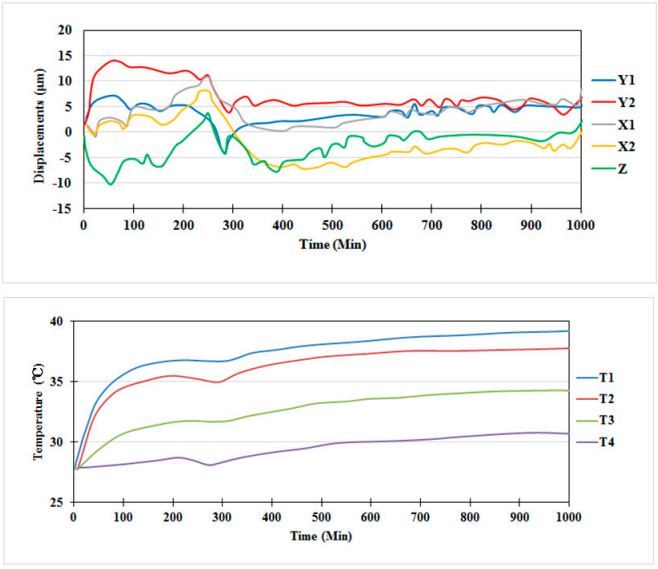


**Figure 13.** Temperature and displacement variations on the *x*-, *y*-, and *z*-axes controlled by the modified compensation system.

### *4.3. Machining Test*

After several times testing of the compensation system, the displacement variations on the *x*- and *y*-axes was controlled to be less than 20 μm, and the displacement variation of the spindle tool center point (TCP) also was controlled within in 20 μm. Finally, we conducted the machining test to verify performance of the compensation system in machining applications. The workpiece material is aluminum with the size of 200 mm × 200 mm × 50 mm. The cutter is a three flute carbide ball end mill with radius of 3 mm and length of 120 mm. The machined parts are shown in Figure 14. A detailed visual examination reveals that the workpiece machined under the activation of the compensation system shows a finished surface, but there are some stripes on the workpiece machined without thermal compensation. The surface accuracy was further examined for workpieces under machining with and without the activation of the thermal compensation system. The surface accuracy of the machined parts without thermal compensation is −25 μm (minimum) and 21 μm (maximum). Figure 14b is machined parts under compensation and the surface accuracy is −14 μm (minimum) and 1 μm (maximum). The overall efficiency is increased by 33%. This result indeed demonstrates the feasibility of the compensation module for reducing the thermal errors in practical machining applications.

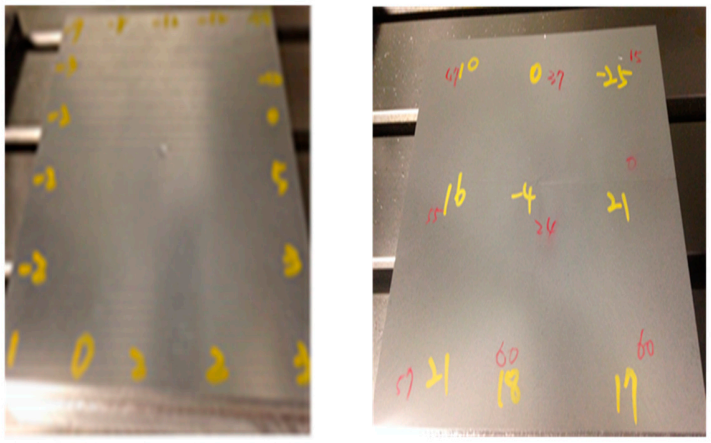

(**a**) (**b**)

**Figure 14.** Machined surface (**a**) without compensation (**b**) with compensation.

## 5. Conclusions

This study aimed to develop a compensation system for controlling the thermal induced positioning error of a CNC milling machine. The compensation system based on the data-driven thermal model was implemented on a milling machine and then verified through the machining test. According to the results, some conclusions can be drawn as follows:

1. Selection of the locations for sensing the temperature fields of the machine tool is very important for establishing the correct thermal model. We first used 14 temperature sensors to examine the real temperature fields around the machine, from which the four major sensing points were selected.
2. Through the proposed thermal compensation system, the displacement variations on the *x*- and *y*-axes and the position error at the tool center can be controlled within 20 μm.
3. Application of the thermal compensation system in milling operation examinations of the machined surface reveal that the surface accuracy can be controlled within −14 μm (minimum) and 1 μm (maximum) under the activation of the compensation system. Compared with the machined surface without thermal compensation, the overall efficiency is increased by 33%. The feasibility of the compensation system was successfully demonstrated in application in the milling operation.

Finally, the proposed compensation system was developed for a three-axis milling machine. For application on four- or five-axis machine tools, the thermal model should be established following the proposed method. However, this would be a hard task since there are more heat sources in the rotary table and swivel head to be examined, which may cause the displacement errors of the rotational axis. This will be part of our future studies and experiments on multiple-axis machine tools.

**Acknowledgments:** The authors would like to acknowledge the support of Quaser Machine Tools Inc. The assistance with the experiment from the Precision Machinery Research & Development Center (PMC) in Taiwan is also highly appreciated.

**Author Contributions:** Tsung-Chia Chen contributed to the organization of the research work, including the experimental configuration, compensation module and manuscript preparation. Chia-Jung Chang and Jui-Pin Hung contributed to the experiment measurements and data analysis. Rong-Mao Lee and Cheng-Chi Wang conducted the experimental work of the machining systems.

**Conflicts of Interest:** The authors declare no conflict of interest.

## References

1. Bryan, J.B. International status of thermal error research. *CIRP Ann. Manuf. Technol.* **1990**, *39*, 645–656. [CrossRef]
2. Ferrreira, P.M.; Liu, C.R. A method for estimating and compensating quasistatic errors of machine tools. *Trans. ASME J. Eng. Ind.* **1993**, *115*, 149–159. [CrossRef]
3. Yanga, H.; Ni, J. Dynamic neural network modelling for nonlinear, nonstationary machine tool thermally induced error. *Int. J. Mach. Tools Manuf.* **2005**, *45*, 455–465. [CrossRef]
4. Zhang, Y.M.; Liu, Q.W.; Han, J.L. Finite element analysis on thermal characteristic of the headstock of NC machine tool. *Adv. Mater. Res.* **2011**, *291–294*, 2302–2305. [CrossRef]
5. Zhang, J.F.; Feng, P.F.; Wu, Z.J.; Yu, D.W.; Chen, C. Thermal structure design and analysis of a machine tool headstock. *Mechanics* **2013**, *19*, 478–485. [CrossRef]
6. Donmez, M.A.; Hahn, M.H.; Soons, J.A. A novel cooling system to reduce thermally-induced errors of machine tools. *CIRP Ann. Manuf. Technol.* **2007**, *56*, 521–524. [CrossRef]
7. Kishawy, H.A.; Dumitrescu, M.; Ng, E.G.; Elbestawi, M.A. Effect of coolant strategy on tool performance, chip morphology and surface quality during high-speed machining of A356 aluminum alloy. *Int. J. Mach. Tools Manuf.* **2005**, *45*, 219–227. [CrossRef]
8. Kodera, T.; Yokoyama, K.; Miyaguchi, K.; Nagai, Y.; Suzuki, T.; Masuda, M.; Yazawa, T. Real-time estimation of ball-screw thermal elongation based upon temperature distribution of ball-screw. *JSME Int. J. Ser. C Mech. Syst.* **2004**, *47*, 1175–1181. [CrossRef]
9. Kim, S.K.; Cho, D.W. Real-time estimation of temperature distribution in a ballscrew system. *Int. J. Mach. Tools Manuf.* **1997**, *37*, 451–464. [CrossRef]
10. Yuan, J.; Ni, J. The real-time error compensation technique for CNC machining systems. *Mechatronics* **1998**, *8*, 359–380. [CrossRef]
11. El Ouafi, A.; Guillot, M.; Barka, N. An integrated modeling approach for ANN-based real-time thermal error compensation on a CNC turning center. *Adv. Mater. Res.* **2013**, *664*, 907–915. [CrossRef]
12. Yang, J.; Yuan, J.; Ni, J. Thermal error mode analysis and robust modeling for error compensation on a CNC turning center. *Int. J. Mach. Tools Manuf.* **1999**, *39*, 1367–1381. [CrossRef]
13. Donmez, M.A.; Blomquist, D.S.; Hocken, R.J.; Liu, C.R.; Barash, M.M. A general methodology for machine tool accuracy enhancement by error compensation. *Precis. Eng.* **1986**, *8*, 187–196. [CrossRef]
14. Chen, J.S.; Yuan, J.; Ni, J.; Wu, S.M. Real-time compensation for time-variant volumetric errors on a machining center. *Trans. ASME J. Eng. Ind.* **1993**, *115*, 472–479. [CrossRef]
15. Lo, C.H.; Yuan, J.; Ni, J. An application of real-time error compensation on a turning center. *Int. J. Mach. Tools Manuf.* **1995**, *35*, 1669–1682. [CrossRef]
16. Lee, D.S.; Choi, J.Y.; Choi, D.H. ICA based thermal source extraction and thermal distortion compensation method for a machine tool. *Int. J. Mach. Tools Manuf.* **2003**, *43*, 589–597. [CrossRef]
17. Postlethwaite, S.R.; Allen, J.P.; Ford, D.G. The use of thermal imaging, temperature and distortion models for machine tool thermal error reduction. *Proc. Inst. Mech. Eng. B J. Eng. Manuf.* **1998**, *212*, 671–679. [CrossRef]

18. Vanherck, P.; Dehaes, J.; Nuttin, M. Compensation of thermal deformation in machine tools with neural nets. *Comput. Ind.* **1997**, *33*, 119–125. [CrossRef]
19. Lee, J.H.; Lee, J.H.; Yang, S.H. Thermal error modeling of a horizontal machining center usingfuzzy logic strategy. *J. Manuf. Process.* **2001**, *3*, 120–127. [CrossRef]
20. Abdulshahed, A.M.; Longstaff, A.P.; Fletcher, S.; Myers, A. Application of GNNMCI(1, N) to environmental thermalerror modelling of CNC machine tools. In Proceedings of the 3rd International Conference on Advanced Manufacturing Engineering and Technologies, Stockholm, Sweden, 27–30 October 2013; pp. 253–262.
21. Abdulshahed, A.M.; Longstaff, A.P.; Fletcher, S.; Myers, A. Comparative study of ANN and ANFIS prediction models for thermal error compensation on CNC machine tools. In Proceedings of the Laser Metrology and Machine Performance X: Lamdamap 10th International Conference, Buckinghamshire, UK, 20–21 March 2013; pp. 79–88.
22. Abdulshahed, A.M.; Longstaff, A.P.; Fletcher, S. A novel approach for ANFIS modelling based on Grey system theory for thermal error compensation. In Proceedings of the 14th UK Workshop on Computational Intelligence (UKCI), Bradford, UK, 8–10 September 2014.
23. Abdulshahed, A.M.; Longstaff, A.P.; Fletcher, S. A particle swarm optimisation-based Grey prediction model for thermal error compensation on CNC machine tools. In Proceedings of the Laser Metrology and Machine Performance XI: 11th International Conference and Exhibition on Laser Metrology, Machine Tool, CMM and Robotic Performance (Lamdamap), Huddersfield, UK, 17–18 March 2015.
24. Horejš, O.; Mareš, M.; Novotný, L. Advanced modelling of thermally induced displacements and its implementation into standard CNC controller of horizontal milling center. *Procedia CIRP* **2012**, *4*, 67–72. [CrossRef]
25. Chen, J.S.; Chiou, G. Quick testing and modeling of thermally-induced errors of CNC machine tools. *Int. J. Mach. Tools Manuf.* **1995**, *35*, 1063–1074. [CrossRef]
26. Kurtoglu, A. The accuracy improvement of machine tools. *Ann. CIRP* **1990**, *39*, 417–419. [CrossRef]
27. Hao, W.; Hongtao, Z.; Qianjian, G.; Xiushan, W.; Jianguo, Y. Thermal error optimization modeling and real-time compensation on a CNC turning center. *J. Mater. Process. Technol.* **2008**, *207*, 172–179. [CrossRef]
28. Yang, S.; Yuan, J.; Ni, I. The improvement of thermal error modeling and compensation on machinetools by CMAC neural network. *Int. J. Mach. Tools Manuf.* **1996**, *36*, 527–537. [CrossRef]
29. Vyroubal, J. Compensation of machine tool thermal deformation in spindle axis direction based on decomposition method. *Precis. Eng.* **2012**, *36*, 121–127. [CrossRef]
30. Abdulshahed, A.M.; Longstaff, A.P.; Fletcher, S.; Myers, A. The application of ANFIS prediction models for thermal error compensation on CNC machine tools. *Appl. Soft Comput.* **2015**, *27*, 158–168. [CrossRef]
31. Abdulshahed, A.M.; Longstaff, A.P.; Fletcher, S.; Myers, A. Thermal error modelling of machine tools based on ANFIS with fuzzy c-means clustering using a thermal imaging camera. *Appl. Math. Model.* **2015**, *39*, 1837–1852. [CrossRef]